Clinical Cancer Research

An Integrated Approach Identifies Mediators of Local Recurrence in Head and Neck Squamous Carcinoma

Francesca Citron[1], Joshua Armenia[1], Giovanni Franchin[2], Jerry Polesel[3], Renato Talamini[3], Sara D'Andrea[1], Sandro Sulfaro[4], Carlo M. Croce[5], William Klement[6], David Otasek[6], Chiara Pastrello[6], Tomas Tokar[6], Igor Jurisica[6,7,8], Deborah French[9], Riccardo Bomben[10], Emanuela Vaccher[11], Diego Serraino[3], Barbara Belletti[1], Andrea Vecchione[5,9], Luigi Barzan[12], and Gustavo Baldassarre[1]

Abstract

Purpose: Head and neck squamous cell carcinomas (HNSCCs) cause more than 300,000 deaths worldwide each year. Locoregional and distant recurrences represent worse prognostic events and accepted surrogate markers of patients' overall survival. No valid biomarker and salvage therapy exist to identify and treat patients at high-risk of recurrence. We aimed to verify if selected miRNAs could be used as biomarkers of recurrence in HNSCC.

Experimental Design: A NanoString array was used to identify miRNAs associated with locoregional recurrence in 44 patients with HNSCC. Bioinformatic approaches validated the signature and identified potential miRNA targets. Validation experiments were performed using an independent cohort of primary HNSCC samples and a panel of HNSCC cell lines. *In vivo* experiments validated the *in vitro* results.

Results: Our data identified a four-miRNA signature that classified HNSCC patients at high- or low-risk of recurrence. These miRNAs collectively impinge on the epithelial–mesenchymal transition process. *In silico* and wet lab approaches showed that miR-9, expressed at high levels in recurrent HNSCC, targets SASH1 and KRT13, whereas miR-1, miR-133, and miR-150, expressed at low levels in recurrent HNSCC, collectively target SP1 and TGFβ pathways. A six-gene signature comprising these targets identified patients at high risk of recurrences, as well. Combined pharmacological inhibition of SP1 and TGFβ pathways induced HNSCC cell death and, when timely administered, prevented recurrence formation in a preclinical model of HNSCC recurrence.

Conclusions: By integrating different experimental approaches and competences, we identified critical mediators of recurrence formation in HNSCC that may merit to be considered for future clinical development. *Clin Cancer Res; 23(14); 3769–80. ©2017 AACR.*

Introduction

Head and neck squamous cell carcinomas (HNSCCs) comprehend a relatively common group of neoplasms, with about 550,000 new cases/year worldwide (1). Most patients are diagnosed with a locally advanced potentially curable cancer, but 40% to 60% of these patients eventually recur (2, 3). A recent meta-analysis demonstrated that the combination of chemo- and radiotherapy is a valid, although highly toxic, therapeutic option (4). Despite this aggressive schedule, the 5-year survival of patients with HNSCC ranges from 35% to 55% (4).

Local and distant recurrences represent valid surrogate endpoints to estimate the efficacy of radiotherapy and chemotherapy on patients' survival (5). This observation implies that identifying patients that will recur could be extremely beneficial for the management of patients with HNSCC to avoid unnecessary toxicity and improve patients' survival. To date, no validated biomarkers exist to identify patients with HNSCC with higher

[1]Division of Molecular Oncology, CRO Aviano, National Cancer Institute, Aviano, Italy. [2]Oncologic Radiotherapy, CRO Aviano, National Cancer Institute, Aviano, Italy. [3]Cancer Epidemiology, CRO Aviano, National Cancer Institute, Aviano, Italy. [4]Division of Pathology, Azienda Ospedaliera Santa Maria degli Angeli, Pordenone, Italy. [5]Department of Cancer Biology and Genetics/CCC, The Ohio State University, Columbus, Ohio. [6]Princess Margaret Cancer Centre, University Health Network, Toronto, Ontario, Canada. [7]Departments of Medical Biophysics and Computer Science, University of Toronto, Canada. [8]Institute of Neuroimmunology, Slovak Academy of Sciences, Bratislava, Slovakia. [9]Faculty of Medicine and Psicology, Department of Clinical and molecular Medicine, University of Rome "La Sapienza," Santo Andrea Hospital, Rome, Italy. [10]Clinical and Experimental Onco-Hematology Unit, CRO Aviano, National Cancer Institute, Aviano, Italy. [11]Medical Oncology, CRO Aviano, National Cancer Institute, Aviano, Italy. [12]Department of Surgery, CRO Aviano, National Cancer Institute, Aviano, Italy.

Note: Supplementary data for this article are available at Clinical Cancer Research Online (http://clincancerres.aacrjournals.org/).

F. Citron and J. Armenia contributed equally to this article.

Current address for J. Armenia: Memorial Sloan Kettering Cancer Center, New York, NY; and current address for W. Klement, Latner Thoracic Surgery Research Laboratory, University Health Network, Toronto, Ontario, Canada.

Corresponding Authors: Gustavo Baldassarre, Centro di Riferimento Oncologico National Cancer Institue, Via Gallini 2, Aviano, PN 33081, Italy. Phone 3904-3465-9779; Fax: 3904-3465-9428; E-mail: gbaldassarre@cro.it; Andrea Vecchione, andrea.vecchione@uniroma1.it; and Luigi Barzan, luigibarzan@libero.it

doi: 10.1158/1078-0432.CCR-16-2814

Translational Relevance

Most patients with HNSCC are diagnosed with a locally advanced disease and are treated with the combination of surgery, radiotherapy, and chemotherapy. This highly toxic approach is curative in about half of the cases, but recurrent patients do not have effective salvage therapies. Therefore, there is the urgency to identify and validate solid biomarkers able to classify patients at high risk that may benefit for specific targeted approaches. Our work tackled these two unmet clinical needs and identified a microRNAs signature of locoregional recurrence in patients with HNSCC. Starting from this signature, we identified two druggable pathways (i.e., SP1 and TGFβ) that when timely and concomitantly targeted efficiently prevented recurrence formation in a preclinical model. Both SP1 and TGFβ inhibitors have been already used to treat human patients; thus, our work is of potential immediate translational relevance.

probability to develop recurrences and that, therefore, may merit a closer follow-up or different therapeutic approaches (6).

HNSCC progression is a stepwise process, resulting from the accumulation of molecular alterations in the squamous epithelium, which eventually drives the progression from premalignant lesions to invasive disease (3). Although inactivation of p53 and RB pathways are considered an early, nearly universal event in HNSCC progression, either through somatic mutation/inactivation of critical tumor suppressor genes (e.g., *TP53* and *CDKN1A*) or through HPV infection (3, 6–8), less is known about the subsequent molecular events necessary for the progression of HNSCC to invasive, metastatic carcinomas. Among others, it has been hypothesized that the regulation of cancer cell plasticity through reversible reprogramming of epithelial-to-mesenchymal transition (EMT) and mesenchymal-to-epithelial transition (MET) could play a primary role (3, 9–12).

Accumulating evidence suggests that EMT favors the distant dissemination of single carcinoma cells from the site of the primary tumor (10, 13) and, more recently, EMT has been proposed as an escape mechanism mediating drug resistance (13). It is therefore conceivable that EMT could play a pivotal role in recurrence formation in HNSCC, either by stimulating local and distant cancer cell spreading or by inducing chemoresistance.

Converging evidence suggests that cancer cell plasticity is regulated epigenetically (11). In this context, miRNAs could play a primary role also in HNSCC (12, 14). After the seminal demonstration that a reciprocal feedback loop exists between the miR-200 family and the ZEB transcription factors to tightly control EMT (15, 16), the number of miRNAs that has been directly or indirectly associated with EMT is becoming an extensive list.

The role of miRNA expression in HNSCC has been widely investigated and several differentially expressed miRNAs in normal/peritumoral mucosa versus primary tumors have been identified (12, 17, 18). However, no study has specifically compared the expression profile of miRNAs in primary tumors from patients who have recurred versus patients that have not.

Here, we report the identification of a 4-miRNAs signature able to identify patients with HNSCC at high risk of recurrence and describe the mechanism whereby they orchestrate the expression of genes regulating cancer cell plasticity via EMT modulation.

Materials and Methods

Patient samples

Specimens from primary HNSCC were collected from patients who underwent surgery at our institution and at Santa Maria degli Angeli Hospital, Pordenone, Italy. HNSCC specimens were immediately frozen and stored at −80°C. The study was approved by the Internal Review Board of the Centro di Riferimento Oncologico (CRO) of Aviano (#IRB-08/2013), and all patients provided written informed consent.

Bioinformatic analyses

Computational analysis. Univariant significance test by the permutation test (19) was used to calculate the statistical significance of each of the four miRNAs individually. Testing of sample classification includes building and testing a computational prediction model to predict recurrence based on the miRNAs' expressions using the Weka software (20). We adopt the undersampling technique described in (21), to counter the effects of class imbalance and the potential of overfitting due to a limited and small minority class data (only 11 recurrent samples). Both methods are further described in the Supplementary Materials and Methods.

Network analysis. After downloading predicted miRNA–gene interactions for the genes in our network from the mirDIP portal ver. 1 (http://ophid.utoronto.ca/mirDIP; ref. 22), which integrates 12 miRNA prediction datasets, we kept only those interactions that were identified in at least three independent datasets. We then integrated the analysis using genes up- or downregulated in head neck recurrences from CDIP, the Cancer Data Integration Portal ver. 1 (http://ophid.utoronto.ca/cdip), a collection of gene expression data from published studies. We also used a list of genes associated with recurrence formation in HNSCC from a published cohort (23).

Next, we uploaded this list of gene IDs into NAViGaTOR 3 as our network visualization tool (http://ophid.utoronto.ca/navigator (24) and retrieved known, publicly available human physical protein interaction using the I2D 2.2 portal (http://ophid.utoronto.ca/i2d (25). Our goal was to explore the relationships between our four miRNAs and genes known to regulate recurrence formation in HNSCC. Network nodes represent miRNAs and proteins respectively, whereas edges represent physical protein–protein interactions (PPI) and miRNA:gene regulation. We downloaded the list of the four miRNAs targets from the mirDIP database ver. 1 (http://ophid.utoronto.ca/mirDIP/) and then we looked at the intersection among genes that control recurrence formation (23), genes associated to a prosurvival signature (23) and the four miRNAs targets.

PathDIP analyses. We analyzed 56 genes, involved in recurrence formation (23), as potential miR-9 targets. These pathway analyses were conducted using pathDIP Ver. 2.4.3.12 (http://ophid.utoronto.ca/pathDIP; ref. 26).

Analysis of the TCGA dataset. Correlation analysis using HNSCC TCGA RNAseq and microRNA-seq data for *SASH1*, *KRT13*, and hsa-miR-9 were performed using Spearman correlation (27). All statistical analyses were performed using [R] (https://www.r-proj

ect.org/). *KRT13/SASH1* correlation analysis using HNSCC TCGA RNAseq data were performed using cBioPortal for Cancer Genomics (http://www.cbioportal.org/; ref. 28).

Clustering of RNAseq values was performed using Ward linkage. This approach identified cluster 1 with high expression of *KRT13/SASH1* and low expression of *TGFβR1/2*, *SMAD3*, and *SP1*, whereas cluster 2 is characterized by high expression of *TGFβR1/2*, *SMAD3*, *SP1*, and low expression of *SASH1/KRT13*. The associations of the two clusters with survival was evaluated with the log-rank test using the survival package in R. HNSCC TCGA patients were stratified either by high mRNA expression of *KRT13/SASH1* and low *SMAD3* (above median of mRNA expression, below median of mRNA expression, respectively) or by high mRNA expression of *SMAD3* and low mRNA expression of *KRT13/SASH1*. Cox proportional hazards regression analysis based on the *KMsurv* package in R was used to assess the hazard ratios. All HNSCC TCGA data were downloaded using the TCGA data portal (https://gdc.cancer.gov/) and the cBioPortal for Cancer Genomics (http://www.cbioportal.org/).

To validate prognostic properties of the four-miRNAs signature, we used SurvMicro v.0.9 (http://bioinformatica.mty.itesm.mx:8080/Biomatec/Survmicro.jsp; ref. 29). Signature was validated on TCGA LUAD Ilumina HiSeq dataset, comprising 311 patient samples. All settings were used as default.

Wet lab analyses

All wet lab analyses were performed according to procedures commonly used in our lab (30, 31) and are described in detail in the Supplementary Materials and Methods.

Molecular biology experiments. miRNA expression profile was performed using the NanoString technology (NanoString nCounter Human miRNA assay (v1.1) that allowed to evaluate the expression of 746 miRNAs (664 Human 82 Viral) along with the one of housekeeping genes (GeneBank GSE89000). NanoString technology, DNA and RNA extraction, quantification and analysis, evaluation of *TP53* and HPV status, protein extraction, and Western blotting are described in the Supplementary Materials and Methods.

Cell culture, transfection, and transduction. All cell lines were authenticated by BMR Genomics srl Padova, Italia according to Cell ID System (Promega) protocol and using Genemapper ID Ver 3.2.1, to identify DNA STR profiles. UMSCC74b and UMSCC1 cells were kindly provided by Dr. Thomas Carey (University of Michigan, Ann Arbor, MI). All other head and neck squamous cell lines were obtained from ATCC (LGC Standards).

Xenograft growth in mouse flanks and treatment. Animal experimentation was approved by the Italian Ministery of Health and by a local ethic committee for animal welfare (OPBA) and experiments performed according to committee's guidelines. Athymic nude mice (Harlan, Foxn1^{nu}, females, 6 weeks old) were injected with 2×10^6 FaDu cells bilaterally in the flanks. The evaluation of local relapse and the administration on Mythramicin A and SB-525334 are provided in the Supplementary Materials and Methods.

Statistical analyses

All graphs and statistical analyses were performed using PRISM (version 6, GraphPad, Inc.) and R, SAS Software 9.2 and R for statistical analyses. In all experiments, differences were considered significant when P was <0.05. Statistical analyses included paired and unpaired t tests, Mann–Whitney unpaired t test and Spearman correlation test, used as appropriate and as specified in each figure. Differences in miRNA expression between patients' groups were evaluated by nonparametric Wilcoxon test (two groups) or Kruskal–Wallis test (three groups). Correlation between Array and PCR quantification of miRNAs was evaluated through Spearman correlation coefficient.

Results

Identification of miRNAs differentially expressed in recurrent and nonrecurrent HNSCC

Primary HNSCC fresh-frozen surgical samples collected from 44 patients (Table 1) who experienced ($n = 11$) or not ($n = 33$) local recurrence within 2 years from the first surgery were analyzed by NanoString technology for the expression of 746 human and 82 viral miRNAs. Statistical analyses of normalized miRNA expression demonstrated that seven miRNAs were significantly different between the two groups (data not shown). Validation of these data by qRT-PCR analyses confirmed significant differences for miR-1, miR-133a, miR-150, and miR-9 between recurrent and nonrecurrent HNSCC. In particular, univariant significance testing confirmed that miR-9 was upregulated, whereas miR-1, miR-133a, and miR-150 were downregulated in tumors from recurrent patients (Supplementary Fig. S1). No significant associations were found between expression of these miRNAs and other clinical and biological variables of the tumors, including the presence of *TP53* mutation and the positivity for HPV infection (Table 1; Supplementary Table S1). Accordingly, miR-9 upregulation and miR-1, miR-133a, and miR-150 downregulation in recurrent tumors was also confirmed when only *TP53* mutant or HPV-negative cases were considered (Supplementary Fig. S1). Bioinformatic validation by data reiteration confirmed the significance of this interaction (Fig. 1A and B; Supplementary Fig. S2). Using the classifier testing, we calculated the AUC to estimate the ability of the four miRNAs, each one alone or in combination, to predict recurrence. Models 1–4, built using a Naïve Bayes or a logistic regression models, in which the classifier combines miR-133a with miR-150, with or without miR-9, achieved a high AUC (80–81%), high sensitivity (82–88%), and low false-positive rates (29%–35%), which translated into 65% to 71% specificity (Fig. 1A and B; Supplementary Fig. S2). Our analyses also suggested that the addition of miR-1 does little to improve the classification accuracy (Supplementary Fig. S2C).

These computational analyses are in accord with the notion that miR-1 and miR-133a belongs to the same cluster (32) and, consequently, their expression highly correlates, as we observed in our samples set (Spearman correlation value $r = 0.9621$; $P < 0.0001$). Correlation analyses also indicated that miR-133a expression directly correlates with miR-150 (Spearman correlation value $r = 0.2984$; $P = 0.049$) and that miR-9 expression inversely correlates with both miR-133a (Spearman correlation value $r = -0.1715$; $P =$ n.s.) and miR-150 (Spearman correlation value $r = -0.4757$ and $P = 0.0011$).

Accordingly, using the HNSCC TCGA dataset (27) we confirmed that (i) miR-1 and -133a expression strongly correlate ($R = 0.79$; $P < 0.0001$); (ii) miR-9 inversely correlates with both miR-1 ($R = -0.27$; $P < 0.0001$) and miR-133a ($R = -0.34$; $P < 0.0001$); and (iii) the expression of miR-1, -133a, -150, and -9 classify patients at high risk of relapse (Fig. 1C).

Table 1. Distribution of relapsed/not relapsed patients and mean level of miRNA expression according to selected covariates

	Relapsed *n* (%)	Not relapsed *n* (%)	miR-9	miR-1	miR-133a	miR-150
Sex						
Men	11 (100.0)	24 (72.7)	319.0	2193.8	396.7	537.7
Women	0 (0.0)	9 (27.3)	180.9	186.5	132.0	1752.8
	$P = 0.0849$		$P = 0.6812$	$P = 0.4459$	$P = 0.9266$	$\mathbf{P = 0.0358}$
Age						
<60 years	8 (72.7)	15 (46.9)	310.8	512.3	86.2	542.4
≥60 years	3 (27.3)	17 (53.1)	288.2	3777.7	721.0	896.1
	$P = 0.1753$		$P = 0.5217$	$P = 0.6463$	$P = 0.6575$	$P = 0.4025$
Cancer site						
Tongue oral cavity	5 (45.5)	23 (69.7)	149.9	724.8	110.0	684.6
Oropharynx Hypopharynx	5 (45.5)	6 (18.2)	329.9	3425.2	662.3	499.5
Larynx	1 (9.0)	4 (12.1)	648.3	78.7	18.4	1452.2
	$P = 0.2104$		$P = 0.3178$	$P = 0.3296$	$P = 0.5829$	$P = 0.2347$
cT						
T1–T2	3 (27.3)	21 (65.6)	209.0	941.5	169.3	584.8
T3–T4	8 (72.7)	11 (34.7)	341.2	2365.4	446.6	744.9
	$\mathbf{P = 0.0383}$		$P = 0.9737$	$\mathbf{P = 0.0409}$	$P = 0.1021$	$P = 0.9211$
cN						
0	3 (27.3)	13 (40.6)	321.0	5360.7	1024.5	626.5
1–2	8 (72.7)	19 (59.4)	292.2	432.0	72.5	726.6
	$P = 0.4942$		$P = 0.7667$	$P = 0.4503$	$P = 0.4409$	$P = 0.7168$
Adjuvant radio/chemotherapy						
No	6 (54.6)	26 (78.8)	160.0	638.9	126.2	489.1
Yes	5 (45.4)	7 (21.2)	391.6	2763.3	513.9	829.3
	$P = 0.1387$		$P = 0.3709$	$P = 0.9752$	$P = 0.4672$	$P = 0.4043$

The significant differences are shown in bold.
Abbreviations: cN, clinical evaluation of node status; cT, clinical evaluation of tumor size.

Bioinformatic analyses identified miRNA targets involved in the regulation of cell plasticity

Confirmed targets of the identified four miRs impinge on EMT process. Specifically, miR-9 promotes EMT by targeting E-cadherin (33) and miR-1, miR-133, and miR-150, act as EMT suppressors by targeting SLUG (34), SNAIL (35), and ZEB1 (36), respectively.

Because EMT plays a pivotal role in HNSCC progression and recurrence formation (3, 12), we applied the mirDIP (22) and NAVIGaTOR (24) bioinformatic tools to integrate miRNA-target predictions with experimentally determined PPIs from I2D as described (25, 37), focusing on genes regulating EMT.

We first identified 16 possible common targets of miR-1, -133a, and -150 (Fig. 1D). Then, we built an interaction network by integrating these analyses with the genes upregulated in HNSCC, as determined by the TCGA consortium. These analyses led us to the identification of SP1 as a common target of these three miRNAs (data not shown). Refinement of these results, using two other available HNSCC datasets of coding gene signatures that could predict recurrences in HNSCC (23, 38), also identified SP1 (Fig. 1E) together with other genes belonging to the TGFβ and β-catenin pathways, as potential targets of miR-1, -133a, and -150 (Fig. 1F).

A similar approach was used to screen the 1611 potential miR-9 targets. By intersecting these targets with genes associated with EMT negative regulators and HNSCC recurrence formation and/or patients' survival, we defined a complex interaction network that highlighted potential targets altered in HNSCC (data not shown). Further refinement of these analyses led to the identification of Plakoglobin (*JUP1*), *SASH1*, Keratin 13 (*KRT13*), and Filaggrin (*FLG*), as the genes with the highest probability to represent miR-9 targets in recurrent HNSCC (Fig. 1G).

Pathway enrichment analyses using pathDIP (26), to integrate miR-1, -133a, and -150 with miR-9 networks, identified significantly enriched pathways (Supplementary Table S2). The most frequently occurring genes belonged to signal transduction (30 genes; $P < 0.05$), EGFR1 (29 genes; $P = 0.01$), immune system (29 genes; $P < 0.02$), integrin α6β4 (26 genes; $P = 0.001$), TNFα (23 genes; $P = 0.05$), developmental biology (22 genes; $P = 0.02$), and TGFβ signaling (22 genes; $P = 0.04$) pathways. Interestingly, four prognostic genes from the work of Reiss and colleagues (38) are predicted to be regulated by miR-9-5p and miR-150-5p (using an updated mirDIP 3.0.1; http://ophid.utoronto.ca/mirDIP; ref. 22).

Experimental validation of identified miRNAs targets involved in the regulation of EMT

Overall, these analyses suggested that the relative expression of miR-1, -133, -150, and miR-9 could play a functional role in HNSCC progression possibly by regulating EMT.

To experimentally validate miRNAs targets identified *in silico*, we screened a panel of HNSCC-derived cell lines for endogenous miRNAs levels to choose the most appropriate *in vitro* model. Generally, all cell lines expressed low levels of miR-1, -133a, and -150 and higher levels of miR-9 (Supplementary Fig. S3A).

First, we focused on the four most probable miR-9 targets, namely *JUP1*, *SASH1*, *KRT13*, and *FLG* (Fig. 1G). FaDu and SCC9 cells expressed highest level of miR-9 and low levels of SASH1, KRT13, and of the epithelial marker E-cadherin (Supplementary Fig. S3A and S3B). In both cell lines, miR-9 knockdown resulted in the upregulation of *SASH1* and *KRT13*, but not of *JUP1* and *FLG* mRNAs (Fig. 2A and Supplementary Fig. S3C and S3D). The increased SASH1 and KRT13 expression was also confirmed at protein level (Fig. 2B). In CAL27 and UMSCC1 cells, expressing low endogenous miR-9, its

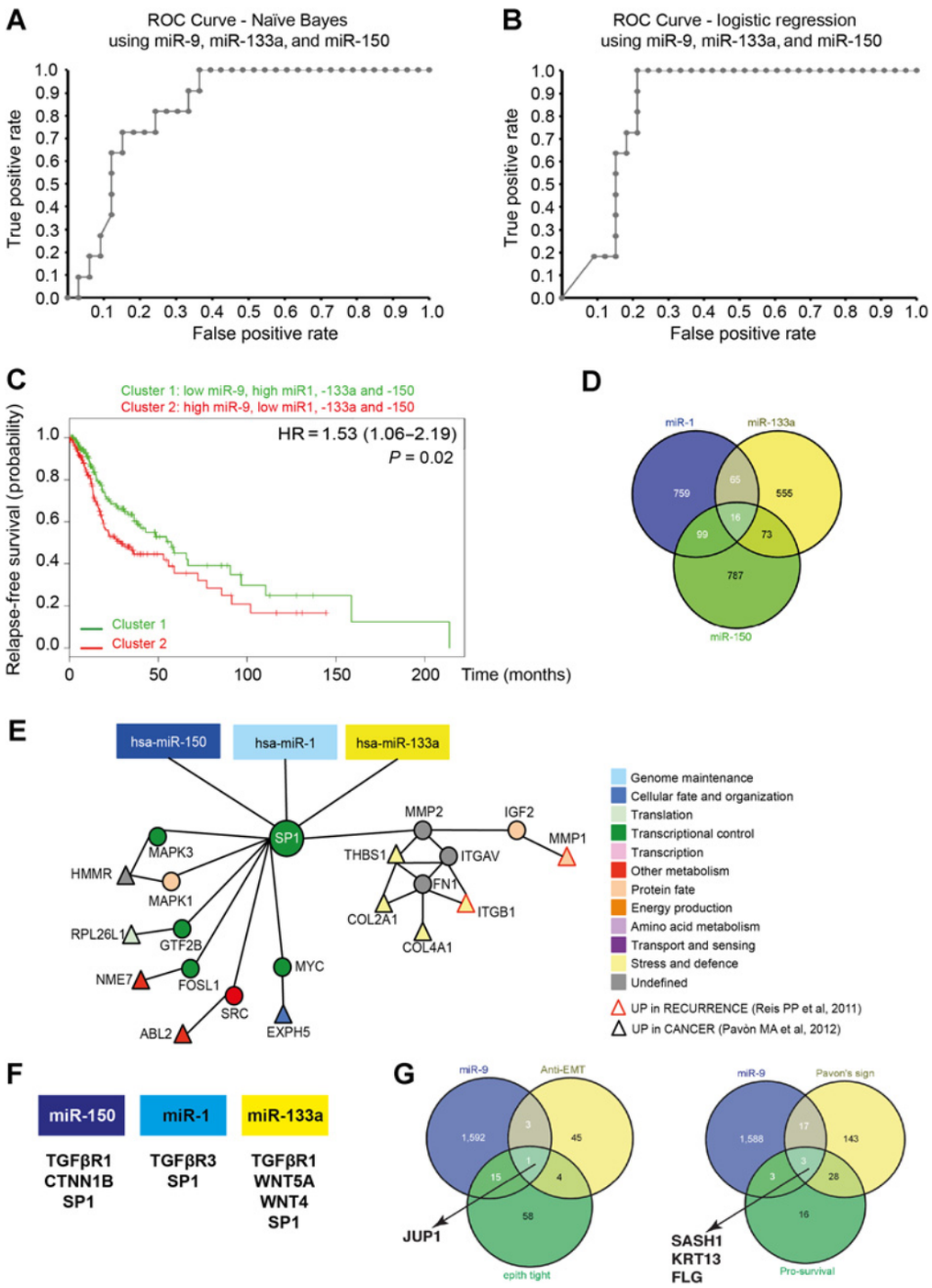

Figure 1.

Identification of miR-1, -133a, -150, and -9 potential targets in HNSCC. ROC curve predicting recurrence formation, using miR-9, -133a, and -150 data iteration, applying the Naïve Bayes (**A**) or the logistic regression (**B**) models. The AUC is 81.3% (sensitivity 87% and specificity 75%) in **A** and 80.3% (sensitivity 82% and specificity 71%) in **B. C,** Kaplan–Meier curve evaluating progression-free survival of patients with HNSCC clustered on the basis of the expression of miR-1, -9, -133a, and -150. **D,** Venn diagram showing the number of miR-1, -133a, and -150 common potential targets, among the EMT genes, altered in HNSCC. **E,** Visualization of miR-1, -133a, and -150 and SP1 network in HNSCC. Direct interactions are shown by edges. Red-border triangles identify genes upregulated in recurrent HNSCC and black-border triangles identify genes upregulated in HNSCC primary tumors. **F,** List of miR-1, -133a, and -150 targets belonging to the TGFβ and WNT pathways. **G,** Venn diagram showing the number of miR-9 potential targets, among the anti-EMT genes and among the genes altered in HNSCC.

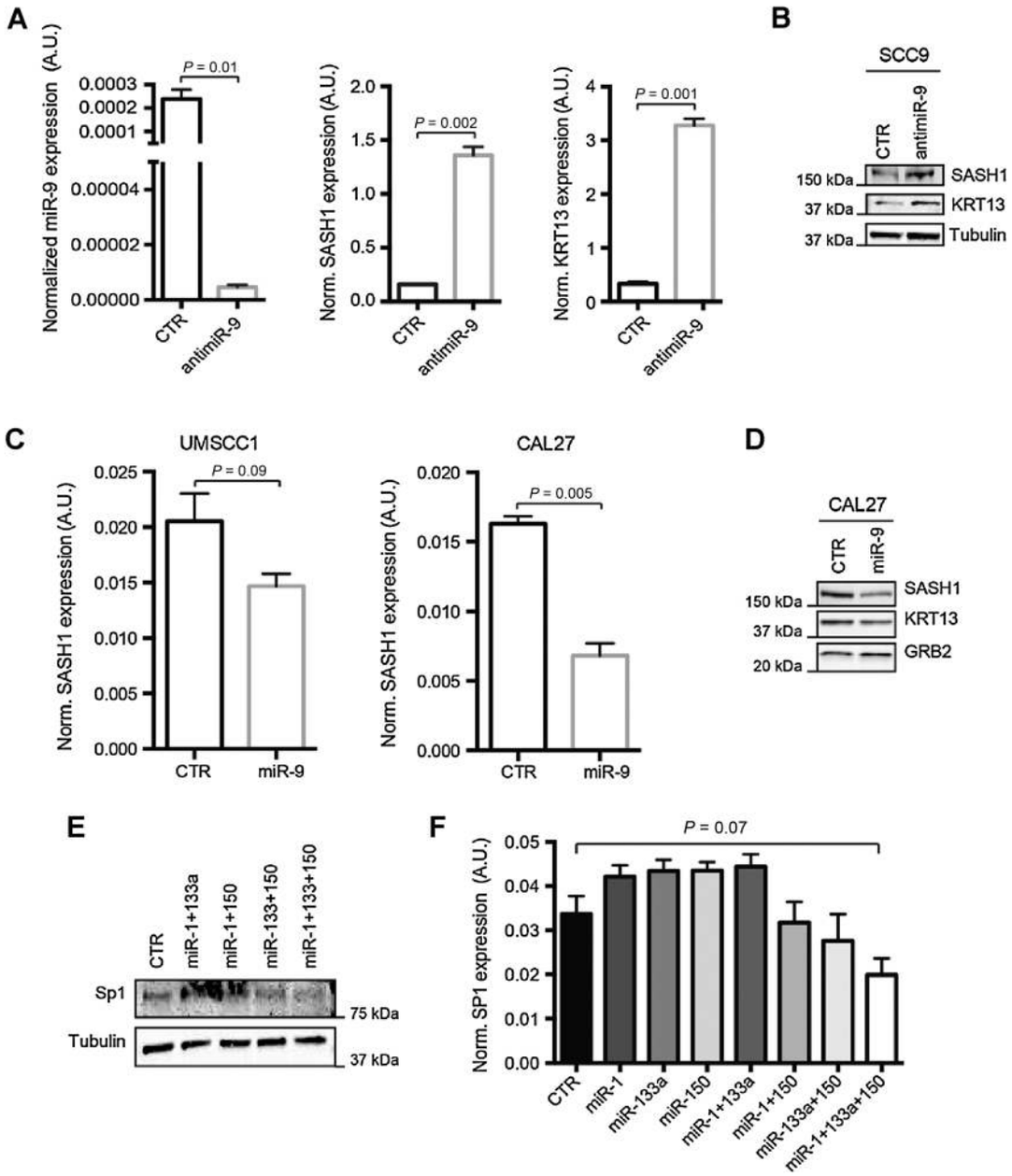

Figure 2.

Validation of SASH1 and KRT13 as miR-9 targets and of SP1 as common target of miR-1, -133a, and -150, in HNSCC cells. **A,** Graphs showing (from left to right) the normalized expression of miR-9, SASH1, and KRT13 RNA in control and miR-9 knockdown SCC9 cells. Data report the median value (±SD) of three independent experiments performed in duplicate. **B,** Western blot analysis of SASH1 and KRT13 protein expressions in control and miR-9 knockdown SCC9 cells. Tubulin was used as loading control. **C,** Graphs showing the normalized expression of SASH1 mRNA expressions in control and miR-9 overexpressing UMSCC1 (left) and CAL27 (right) cells. Graphs report the median value (±SD) of three independent experiments performed in duplicate. **D,** Western blot analysis of SASH1 and KRT13 protein expressions in control and miR-9–overexpressing CAL27 cells. GRB2 was used as loading control. **E,** Western blot analysis of SP1 protein expression in UMSCC74b cells expressing miR-1, -133a, and -150 alone or in combination, as indicated. Tubulin was used as loading control. **F,** Graph showing the normalized expression of SP1 mRNA in UMSCC74b cells transfected as in **E**. Data report the median value (±SD) of three independent experiments performed in duplicate. Statistical significance was calculated using unpaired two-tailed Student *t* test.

overexpression decreased mRNA and protein expression of SASH1 and KRT13 (Fig. 2C and D). As a proof of principle, we also tested whether miR-9 could directly regulate SASH1 expression acting on its 3′-UTR, which contains three seed sites for miR-9 (Supplementary Fig. S4A). Luciferase assay in FaDu cells demonstrated that miR-9 knockdown significantly increased the luciferase activity when the first seed site (position 217–223) was tested (Supplementary Fig. S4B). Overall,

these data suggest that SASH1 (and likely KRT13) could represent reliable markers of miR-9 activity in HNSCC cells.

We next experimentally validated SP1 as common target of miR-1, miR-133a, and miR-150. Overexpression of miR-1, miR-133a, or miR-150 alone did not affect SP1 mRNA or protein expression in different HNSCC cell lines. However, the combined overexpression of two and, even better, of the three miRNAs together significantly reduced SP1, at both protein and mRNA levels (Fig. 2E and F; Supplementary Fig. S5A and S5B). Expression data paralleled luciferase assay on SP1 3′-UTR, which contains one seed site for miR-1 and miR-133a and two seed sites for miR-150 (Supplementary Fig. S4C). Each miRNA alone slightly reduced the luciferase activity of each construct (Supplementary Fig. S4D), further supporting the possibility that the three miRNAs need to work together to reduce SP1 expression.

Members of TGFβ and β-catenin pathways were also predicted targets of miR-1, miR-133a, and miR-150. Among the predicted targets of miR-1, miR-133a, and miR-150 (i.e., *TGFβ-R1*, *TGFβ-R2*, and *TGFβ-R3*, *WNT4*, *WNT5A*, and *CTNN1B*), the expression of *WNT5A* strongly decreased in cells overexpressing miR-133a (Supplementary Fig. S5C), whereas the expression of *TGFβ-R3* decreased following the combined overexpression of the three miRNAs (Supplementary Fig. S5D).

From a functional point of view, we observed that combined inhibition of miR-9 and overexpression of miR-1, -133a, and -150 (Supplementary Fig. S5E) upregulated the epithelial marker E-cadherin in FaDu cells (Supplementary Fig. S5F), supporting the hypothesis that balanced expression of miR-9 and miR-1, miR-133a, and miR-150 plays a functional role in HNSCC recurrence formation by modulating the EMT process.

In vivo validation of identified miRNAs targets involved in the regulation of EMT

To verify if the predicted targets of the four miRNAs were effectively differentially regulated in HNSCC samples, we tested by qRT-PCR the expression *SP1*, *TGFβ-R1*, *TGFβ-R2*, and *TGFβ-R3*, *WNT4* and *WNT5A*, *CTNN1B*, *SASH1*, and *KRT13* in the 44 samples described in Supplementary Table S1 and analyzed for the expression of miRNAs.

In line with *in vitro* results, we observed that miR-9 targets, *SASH1* and *KRT13*, were both significantly downregulated in patients who experienced recurrence (Fig. 3A) and the expression of *SASH1* correlated directly with *KRT13* and inversely with miR-9 in primary HNSCC (Fig. 3B and C). Among miR-1, -133a, and -150 targets, only SP1 and TGFβ-R1 were significantly upregulated in HNSCC samples from recurrent patients (Fig. 3D) and their expression directly correlated (Fig. 3E). No differential expression was observed for *TGFβ-R2* and *TGFβ-R3*, *WNT4*, *WNT5A*, and *CTNN1B* between patients with or without recurrence (data not shown).

To validate our findings in an independent cohort, we collected 78 HNSCC samples in our Institutes (Supplementary Table S3) and evaluated the expression of the four miRNAs, *SASH1*, *KRT13*, *SP1*, and *TGFβR1*. In accord with previous results, miRNAs expression did not correlate with any biological variable of patients with HNSCC, including sex, age, cancer site, T stage, and N stage (Supplementary Table S3).

The expression of *SASH1* inversely correlated with miR-9 and directly correlated with *KRT13* (Supplementary Fig. S6A and S6B). An inverse, although not significant, correlation was noticeable between miR-1 or miR-133a and *SP1* expression, as expected from the *in vitro* results (Supplementary Fig. S6C and S6D).

miRNAs targets predict prognosis in the TCGA HNSCC dataset

We hypothesized that the expression of SASH1, KRT13, SP1, and members of TGFβ pathway could be used in HNSCC as readout of miRNA activity and tested the expression and the correlation of these genes with miR-9 and miR-1, -133a, and -150, in the TCGA dataset.

In accord with the data obtained using our discovery- and validation-cohorts, correlation analyses confirmed that *SP1* positively correlated with miR-9 and inversely with miR-133a (Supplementary Fig. S7A and S7B). Similar results were observed for SMAD2 and SMAD3 expression, used as readouts of SP1 and TGFβ pathway activity (Supplementary Fig. S7C–S7H). Moreover, *SASH1* expression directly correlated with *KRT13* (Supplementary Fig. S7I) and both were higher in tumor-free cohort (Supplementary Fig. S7L).

Cluster analyses, using the expression of *SASH1*, *KRT13*, *SP1*, *TGFβR1*, *TGFβR2*, *SMAD2*, and *SMAD3*, divided the patients with HNSCC included in the TCGA dataset in two groups: one with low expression of SP1 and members of TGFβ pathway and high expression of *KRT13* and *SASH1* (Cluster 1) and the other with the opposite gene expression profile (Cluster 2; Fig. 4A). This clustering had prediction power, because patients included in Cluster 2 displayed worse relapse-free survival than patients included in Cluster 1 (HR 2.01; 95% CI, 1.1–3.8; $P = 0.01$; Fig. 4B).

Perisurgical treatment with SP1 and TGFβR1 inhibitors prevents local relapse in a xenograft model of HNSCC

The above data suggested that SP1 and TGFβ pathway could act together in the establishment of recurrence in patients with HNSCC. To evaluate this possibility, we first tested the *in vitro* efficacy of Mithramycin A (MTA), a validated SP1 inhibitor, and of two different TGFβR1 inhibitors (SB525334, SB52 and SB431542, SB43) on HNSCC cell survival. Although MTA was highly active in decreasing HNSCC cell survival in the nanomolar range, both SB52 and SB43 did not significantly affect cell survival, when used up to 100 μmol/L (Fig. 4C). Yet, in all tested cell lines SB52, used at the ineffective dose of 40 μmol/L, reduced by the half the IC_{50} of MTA (Fig. 4C), suggesting that they could have synergistic effects. Accordingly, MTA used at the concentration of 20 nmol/L effectively induced PARP1 cleavage (marker of apoptosis) only in combination with SB52 or SB43 (40 μmol/L) in FaDu cells (Fig. 4D).

On the basis of these results, we tested if combined pharmacological inhibition of SP1 and TGFβ pathways could restrain the formation of local recurrences *in vivo*, using a model of HNSCC recurrences and a perisurgical treatment schedule (Fig. 5A). Mice were subcutaneously injected with FaDu cells and tumor mass allowed to grow up to approximately 1 cm^3. Mice were then randomly divided in four groups: (i) sham-treated, (ii) treated with MTA 1 mg/kg, (iii) SB52 15 mg/kg, and (iv) the combination of MTA and SB52. All groups were treated for three consecutive days (day −1, day 0, and day +1, with respect to surgery) and two more doses (day +3 and +6) only for SB52 treatment. Tumors were surgically removed at day 0 and appearance of local recurrence was monitored over the subsequent 8 weeks of follow-up (Fig. 5A). Pathologic analyses of explanted tumors, evaluating the presence and the width of resection margins, demonstrated that no significant differences existed among the four groups in the extent of radical surgery (Fig. 5B).

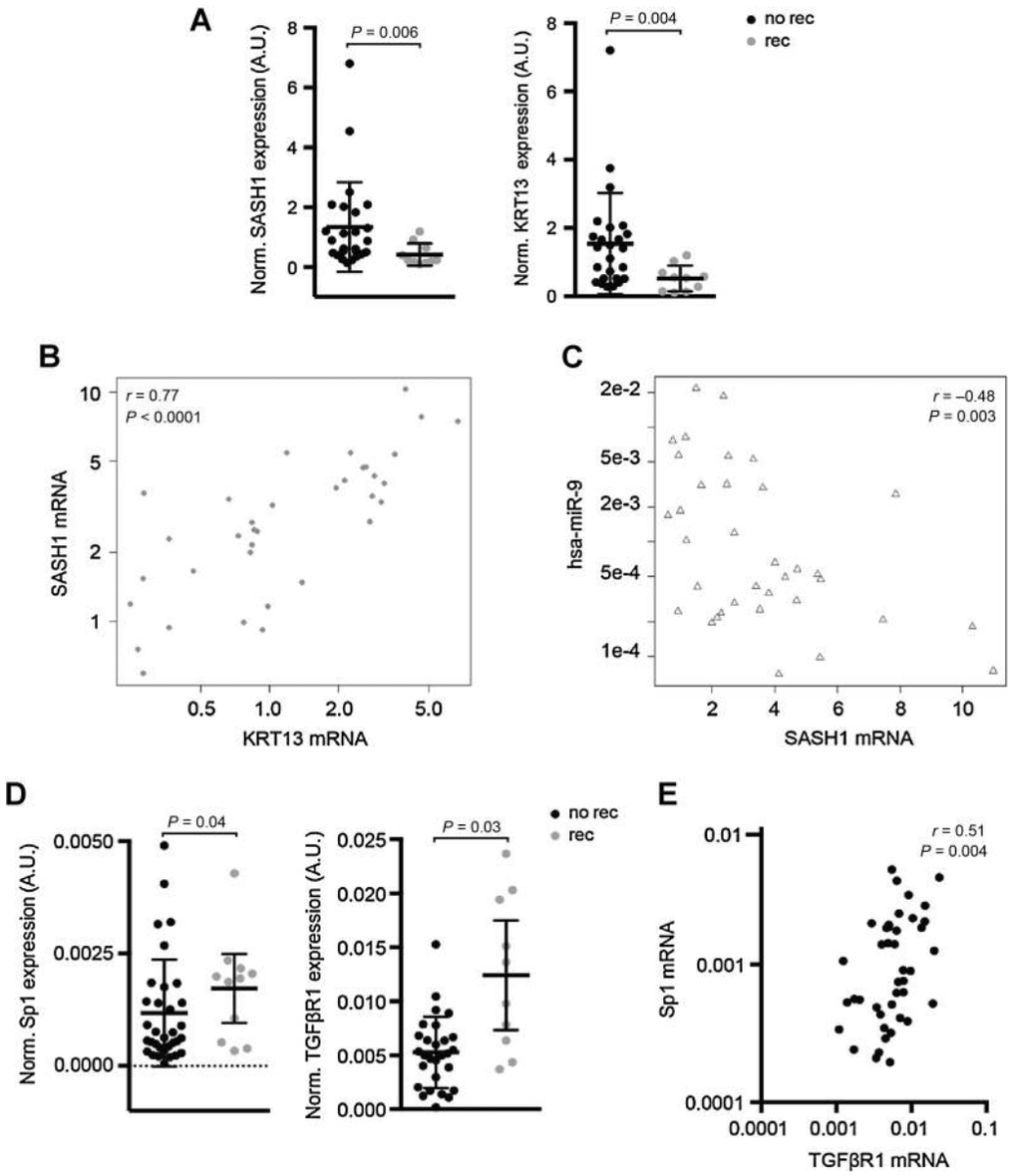

Figure 3.

Expression of identified miRNAs targets in primary HNSCC from recurrent and nonrecurrent patients. **A,** Dot plots showing the normalized expression of SASH1 (left) and KRT13 (right) mRNA, in samples from primary HNSCC from recurrent and nonrecurrent patients. Bars indicate the mean and the 95% confidence interval. Statistical significance was calculated using the Mann–Whitney test. **B** and **C,** Dot plot showing the correlation of SASH1 and KRT13 (**B**) or SASH1 and miR-9 (**C**) mRNA expression in HNSCC samples described in **A**. Correlation value (*r*) and statistical significance (*P*) were calculated using the Spearman correlation test. **D,** Dot plots showing the normalized expression of SP1 (left) and TGFβ-R1 (right) mRNA expressions in samples from primary and recurrent HNSCC samples. Bars indicate the mean and the 95% confidence interval. Statistical significance reported in the graph was calculated using the Mann–Whitney test. **E,** Dot plot showing the correlation of SP1 and TGFβ-R1 mRNA expression in HNSCC samples as in **A**. Correlation value (*r*) and statistical significance (*P*) were calculated using the Spearman correlation test.

Explanted tumors (six from controls and eight per group of treatment, respectively) were analyzed for the expression of phosphorylated SMAD2 (pSMAD2; Fig. 5C and D) and SP1 levels (Fig. 5E), as readouts of SB52 and MTA activity, respectively. A single administration of SB52 and/or MTA (administered the day prior to surgery) significantly inhibited SMAD2 phosphorylation and SP1 expression in the tumors (Fig. 5C–E), confirming the *in vivo* efficacy of these drugs.

Control mice developed local recurrence in 50% of injected sites and MTA used alone did not significantly alter the rate of recurrence formation (4/8, 50%; Fig. 5F). Interestingly, treatment with TGFβR1 inhibitor, SB52, as a single agent considerably increased local recurrence formation, with recurrence occurring in almost all cases (7/8, 90%; Fig. 5F). However, the combination of SB52 + MTA completely prevented recurrence formation (0/8, 0%; $P = 0.005$ in log-rank test; HR 10.01; by comparing control-

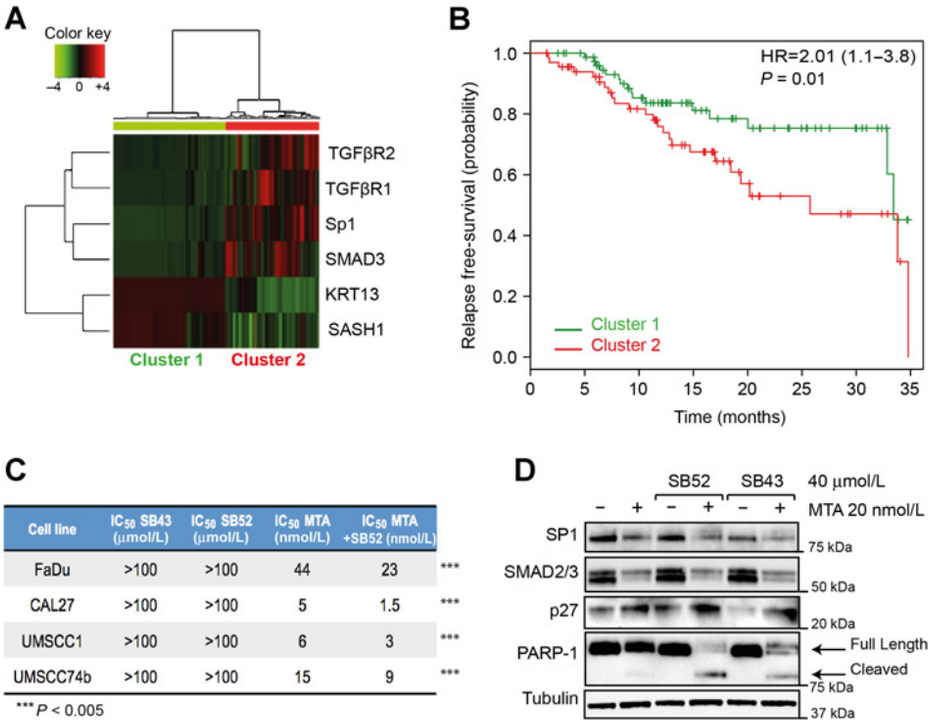

Figure 4.

Expression of miRNAs targets predict prognosis of patients with HNSCC in the TCGA dataset. **A,** Cluster analyses of TGFβR1, TGFβR2, SP1, SMAD3, KRT13, and SASH1 in HNSCC samples included in the TCGA dataset. **B,** Kaplan–Meier curve evaluating progression free survival of patients with HNSCC divided based on the cluster analysis shown in **A**. HR, confidence interval (between brackets), and significance (*P*) were evaluated with the log-rank test using the survival package in R. **C,** Table reports the IC_{50} values of SB431542 (SB43), SB525334 (SB52), and Mithramycin A (MTA) alone or in combination with SB52 (40 μmol/L) in the indicated HNSCC cell lines. Significant difference (***, $P < 0.0001$) between the IC_{50} of MTA, in the presence or not of SB52, was calculated with unpaired two-tailed Student *t* test. **D,** Western blot analysis evaluating the expression of SP1, SMAD2/3 (readouts of MTA activity), p27 (readout of SB52/SB43 activity), and PARP-1 (cleaved form used as marker of apoptosis) in FaDu cells, treated for 24 hours with 20 nmol/L MTA, 40 μmol/L SB52, or SB43 or their combination, as indicated. Tubulin was used as loading control.

and MTA+SB-treated mice; Fig. 5F), suggesting that perisurgical treatment with MTA and SB52 was sufficient to efficiently suppress HNSCC recurrence *in vivo*.

Discussion

Here, we show that four miRNAs can identify in patients with HNSCC those at high risk of developing recurrence. Using multiple approaches, we have linked the activity of these miRNAs to the regulation of EMT, a process considered an critical step in the progression of HNSCC from a pre-invasive to a frankly invasive stage (3). We identified two principal pathways regulated by these miRNAs that likely play a role in the regulation of HNSCC recurrence via the modulation of EMT, the SP1 and the TGFβ pathways. On one side, miR-1, miR-133a, and miR-150 acted together to regulate SP1 and, possibly, TGFβ pathway members, two pathways largely involved in cancer progression and EMT (39, 40). However, miR-9 acted by lowering the expression of *SASH1* and *KRT13*, two known tumor suppressors with potential anti-EMT roles in HNSCC progression (41–43). Using two independent HNSCC samples cohorts and the TCGA datasets, we confirmed the inverse correlation between the identified miRNAs and their targets' expression. This finding supports the possibility that the activity of miR-1, miR-9, miR-133a, and miR-150 could be estimated in primary HNSCC by evaluating the expression of *SP1*, members of the TGFβ pathway, *SASH1* and *KRT13* (our six-gene signature) and that this balanced activity, more than the sole miRNAs expression, could be used as a marker for identifying patients at high risk of developing recurrence.

From a biological point of view, it is interesting to note that we describe here two new targets of miR-9, SASH1 and KRT13, both already linked to the regulation of cell motility and invasion (41, 44). Although the aim of this study was limited to the assessment of their role as potential readouts of high miR-9 activity *in vivo*, it will be worth testing if SASH1 and KRT13 may partially mediate the miR-9-induced local relapse in HNSCC, also in light of the recently proposed role for miR9 in promoting EMT and a cancer stem cell phenotype in squamous cell carcinomas (45).

Importantly, our data point to the simultaneous inhibition of SP1 and TGFβ pathway by the concerted action of three miRNAs, miR-1, miR-133a, and miR-150, as a possible mechanism to prevent disease relapse. At a first glance, our data do not fit in the current literature showing that, in mouse models, the inhibition of TGFβ pathway combined with K-Ras activation is linked to the onset of SCC in the skin and in the oral mucosa (45, 46). However, increasing evidences clearly show that, depending on the stages of tumor progression, TGFβ pathway can exert either pro- or antitumorigenic effects (40). For instance, increased TGFβ signaling, in benign tumors or during the course of cancer

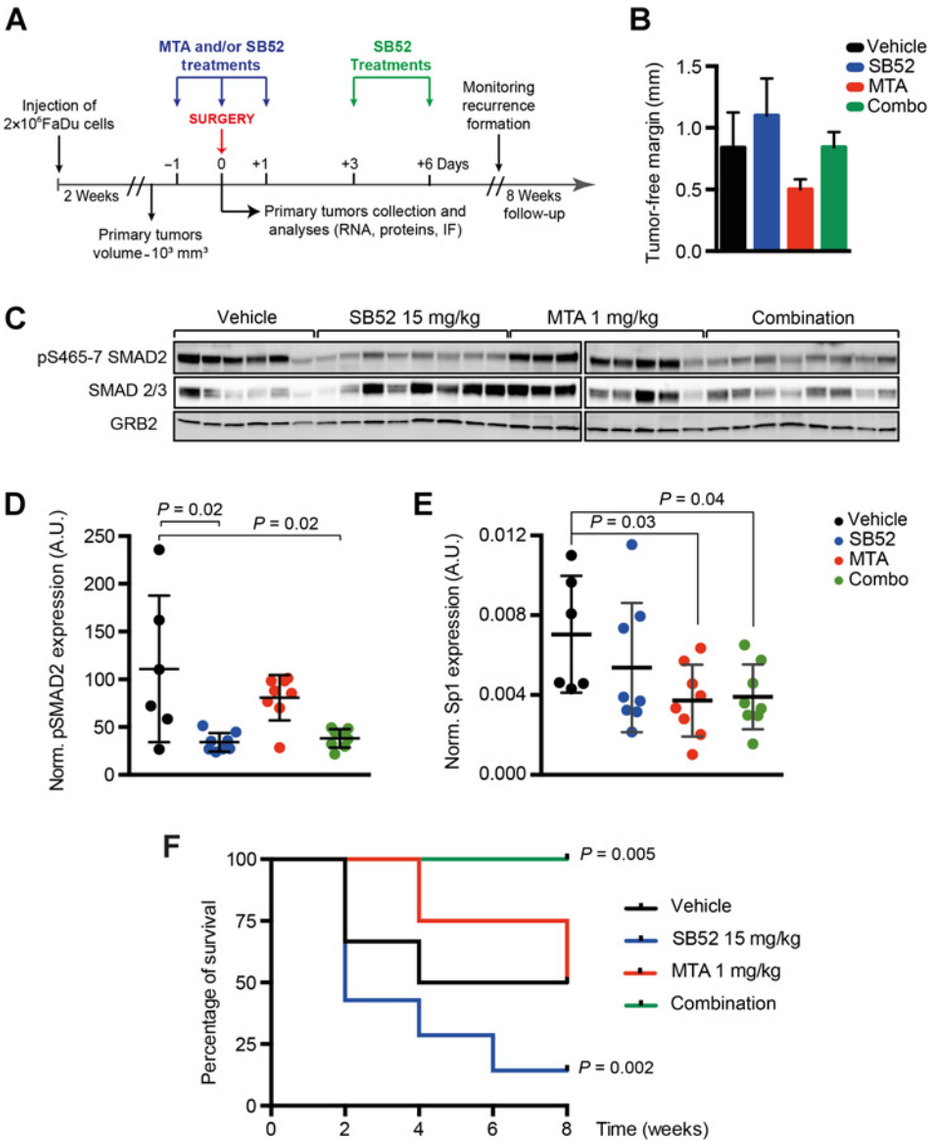

Figure 5.

In vivo inhibition of SP1 and TGFβ pathway effectively reduces recurrence formation in mice. **A,** Schematic representation of the experimental workflow used for the evaluation of recurrence formation in mice xenografted with HNSCC cells. Tumor-bearing mice received the treatments the day before surgery (day −1), the day of surgery (day 0), and the days +1, +3, and +6 after surgery, as indicated. Mice have been then followed up to 8 weeks to monitor recurrence formation. Control mice were treated with the vehicle alone. **B,** The graph reports the evaluation of surgical resection margins in explanted tumors, measured with an optical microscope equipped with an ocular micrometer. Tumor free margins varied from 0.3 to 1.6 mm. No significant differences were observed among the four groups of treatment. **C,** Western blot analysis of tumors explanted from mice treated as described in **A** showing the expression and inhibition of pSMAD2 (S465/7) and SMAD2/3. GRB2 was used as loading control. **D** and **E,** Dot plot reporting the normalized expression of pSMAD2 (S465/7; **D**) or SP1 mRNA (**E**) in tumors explanted at day 0 from mice treated as described in **A**. Each dot in the graph represents a primary tumor that received the one dose of vehicle (black) MTA 1 mg/kg (red), SB52 15 mg/kg (blue), or their combination of MTA + SB52 (green). **F,** Disease-free survival of mice subjected to surgery to remove primary tumors (1,000–1,200 mm^3) and then treated with vehicle (black line), MTA at 1 mg/kg (red line), SB52 15 mg/kg (blue line), or combination of MTA + SB52 (green line). Kaplan—Meier test has been used to calculate the significance of combo-treatment respect to control and to SB52-treated mice.

induction, selects for more aggressive cells and contributes to metastasis formation, in different models of HNSCC (47–49). Our data in the mouse model, showing that TGFβR1 inhibition could result in different outcomes, depending on the simultaneous inhibition of SP1 by MTA or not (Fig. 5F), confirm the hypothesis that TGFβ pathway could act as tumor suppressor or tumor promoter in a context-dependent manner (40, 47). In strict accord with our data, SP1 is required for TGFβ-induced EMT in pancreatic cancer (50), and SP1 and SMAD2 proteins have been reported to directly interact in different models (39), supporting the possibility that SP1 and TGFβ pathway may act together to drive EMT, local invasion and, eventually, recurrence formation in HNSCC. The experimental and *in silico* analyses performed on our and on TCGA samples support this possibility and point to the expression of miR-1, miR-133a, and miR-150 as possible switches of the TGFβ activity.

We are aware that our study has limitations that should be taken into account. The cohort of patients used as a discovery set contains a relatively small number of heterogeneous patients that received different postsurgery treatments. These variables could have an impact on the prognostic value of the miRNA signature and also prevented the possible evaluation of its independent prognostic role in multivariate analyses. Although we experimentally validated the correlation between miRNAs expression and their target, we could not test the potential prognostic value of these miRNAs in a second independent cohort of samples for the absence of a precise follow-up in this group of patients.

Furthermore, it is important to point out that we focused our bioinformatic analyses on the relation between miRNAs expression and EMT regulators, and this represents a possible limitation of our study, since other biological pathways are also significantly altered by the same miRNAs in HNSCC.

In perspective, it will be important to verify if these four miRNAs and/or six genes signatures could be prospectively validated to identify patients at high risk of recurrence who may merit to be treated specific targeted therapies. Because both SP1 and

TGFβ inhibitors have been already tested in cancer patients, our data are of potential immediate translational relevance.

Disclosure of Potential Conflicts of Interest

No potential conflicts of interest were disclosed.

Authors' Contributions

Conception and design: F. Citron, J. Armenia, G. Franchin, R. Talamini, A. Vecchione, L. Barzan, G. Baldassarre

Development of methodology: F. Citron, J. Armenia, S. D'Andrea, T. Tokar, D. French

Acquisition of data (provided animals, acquired and managed patients, provided facilities, etc.): G. Franchin, R. Talamini, S. Sulfaro, C.M. Croce, D. French, E. Vaccher, A. Vecchione, L. Barzan

Analysis and interpretation of data (e.g., statistical analysis, biostatistics, computational analysis): F. Citron, J. Armenia, G. Franchin, J. Polesel, W. Klement, T. Tokar, I. Jurisica, R. Bomben, D. Serraino, B. Belletti, L. Barzan, G. Baldassarre

Writing, review, and/or revision of the manuscript: F. Citron, J. Armenia, G. Franchin, R. Talamini, W. Klement, D. Otasek, C. Pastrello, T. Tokar, I. Jurisica, B. Belletti, A. Vecchione, L. Barzan, G. Baldassarre

Administrative, technical, or material support (i.e., reporting or organizing data, constructing databases): R. Talamini, D. Otasek, C. Pastrello

Study supervision: G. Baldassarre

Acknowledgments

We are grateful to the patients who participated to this study. We thank all members of the SCICC Lab of The Molecular Oncology Unit for supportive scientific discussions.

Grant Support

This work was partially supported by grants from Associazione Italiana Ricerca sul Cancro (AIRC) IG 12854 (to G. Baldassarre) and IG 16862 (to A. Vecchione) and by CRO 5% grant (to G. Baldassarre).

The costs of publication of this article were defrayed in part by the payment of page charges. This article must therefore be hereby marked *advertisement* in accordance with 18 U.S.C. Section 1734 solely to indicate this fact.

Received November 9, 2016; revised December 5, 2016; accepted January 24, 2017; published OnlineFirst February 7, 2017.

References

1. Ferlay J, Shin H-R, Bray F, Forman D, Mathers C, Parkin DM. Estimates of worldwide burden of cancer in 2008: GLOBOCAN 2008. Int J Cancer 2010;127:2893–917.
2. Adelstein DJ, Li Y, Adams GL, Wagner HJr, Kish JA, Ensley JF, et al. An intergroup phase III comparison of standard radiation therapy and two schedules of concurrent chemoradiotherapy in patients with unresectable squamous cell head and neck cancer. J Clin Oncol 2003; 21:92–8.
3. Haddad RI, Shin DM. Recent advances in head and neck cancer. N Engl J Med 2008;359:1143–54.
4. Blanchard P, Baujat B, Holostenco V, Bourredjem A, Baey C, Bourhis J, et al. Meta-analysis of chemotherapy in head and neck cancer (MACH-NC): a comprehensive analysis by tumour site. Radiother Oncol 2011; 100:33–40.
5. Michiels S, Le Maître A, Buyse M, Burzykowski T, Maillard E, Bogaerts J, et al. Surrogate endpoints for overall survival in locally advanced head and neck cancer: meta-analyses of individual patient data. Lancet Oncol 2009; 10:341–50.
6. Hammerman PS, Hayes DN, Grandis JR. Therapeutic insights from genomic studies of head and neck squamous cell carcinomas. Cancer Discov 2015;5:239–44.
7. Stransky N, Egloff AM, Tward AD, Kostic AD, Cibulskis K, Sivachenko A, et al. The mutational landscape of head and neck squamous cell carcinoma. Science 2011;333:1157–60.
8. Agrawal N, Frederick MJ, Pickering CR, Bettegowda C, Chang K, Li RJ, et al. Exome sequencing of head and neck squamous cell carcinoma reveals inactivating mutations in NOTCH1. Science 2011;333:1154–7.
9. Rothenberg SM, Ellisen LW. The molecular pathogenesis of head and neck squamous cell carcinoma. J Clin Invest 2012;122:1951–7.
10. Tsai JH, Yang J. Epithelial-mesenchymal plasticity in carcinoma metastasis. Genes Dev 2013;27:2192–206.
11. Tam WL, Weinberg RA. The epigenetics of epithelial-mesenchymal plasticity in cancer. Nat Med 2013;19:1438–49.
12. Babu JM, Prathibha R, Jijith VS, Hariharan R, Pillai MR. A miR-centric view of head and neck cancers. Biochim Biophys Acta 2011;1816:67–72.
13. Nieto MA, Huang RY-J, Jackson RA, Thiery JP. EMT: 2016. Cell 2016; 166:21–45.
14. Ceppi P, Peter ME. MicroRNAs regulate both epithelial-to-mesenchymal transition and cancer stem cells. Oncogene 2014;33:269–78.
15. Gregory PA, Bert AG, Paterson EL, Barry SC, Tsykin A, Farshid G, et al. The miR-200 family and miR-205 regulate epithelial to mesenchymal transition by targeting ZEB1 and SIP1. Nat Cell Biol 2008;10:593–601.
16. Park S-M, Gaur AB, Lengyel E, Peter ME. The miR-200 family determines the epithelial phenotype of cancer cells by targeting the E-cadherin repressors ZEB1 and ZEB2. Genes Dev 2008;22:894–907.
17. Sethi N, Wright A, Wood H, Rabbitts P. MicroRNAs and head and neck cancer: reviewing the first decade of research. Eur J Cancer 2014;50: 2619–35.
18. Jamali Z, Asl Aminabadi N, Attaran R, Pournagiazar F, Ghertasi Oskouei S, Ahmadpour F. MicroRNAs as prognostic molecular signatures in human head and neck squamous cell carcinoma: a systematic review and meta-analysis. Oral Oncol 2015;51:321–31.
19. Corcoran CD, Senchaudhuri P, Mehta CR, Patel NR. Exact inference for categorical data. 4. Encycl Biostat 2005. doi: 10.1002/0470011815.b2a10019.
20. Hall M, Frank E, Holmes G, Pfahringer B, Reutemann P, Witten IH. The WEKA data mining software: an update. SIGKDD Explorations; 2009; 11:10–18.
21. Klement W, Wilk S, Michalowski W, Matwin S. Classifying severely imbalanced data. In: Butz C, Lingras P, editors. Adv Artif Intell. Berlin/Heidelberg, Germany: Springer Berlin Heidelberg; 2011. p258–64.
22. Shirdel EA, Xie W, Mak TW, Jurisica I. NAViGaTing the micronome–using multiple microRNA prediction databases to identify signalling pathway-associated microRNAs. PLoS One 2011;6:e17429.
23. Pavón MA, Parreño M, Téllez-Gabriel M, Sancho FJ, López M, Céspedes MV, et al. Gene expression signatures and molecular markers associated with clinical outcome in locally advanced head and neck carcinoma. Carcinogenesis 2012;33:1707–16.
24. Brown KR, Otasek D, Ali M, McGuffin MJ, Xie W, Devani B, et al. NAViGaTOR: Network Analysis, Visualization and Graphing Toronto. Bioinformatics 2009;25:3327–9.
25. Brown KR, Jurisica I. Unequal evolutionary conservation of human protein interactions in interologous networks. Genome Biol 2007;8:R95.
26. Rahmati S, Abovsky M, Pastrello C, Jurisica I. pathDIP: an annotated resource for known and predicted human gene-pathway associations and pathway enrichment analysis. Nucleic Acids Res 2017;45:D419–26.
27. The Cancer Genome Atlas Network. Comprehensive genomic characterization of head and neck squamous cell carcinomas. Nature 2015;517: 576–82.
28. Gao J, Aksoy BA, Dogrusoz U, Dresdner G, Gross B, Sumer SO, et al. Integrative analysis of complex cancer genomics and clinical profiles using the cBioPortal. Sci Signal 2013;6:pl1.
29. Aguirre-Gamboa R, Trevino V. SurvMicro: assessment of miRNA-based prognostic signatures for cancer clinical outcomes by multivariate survival analysis. Bioinformatics 2014;30:1630–2.
30. Fabris L, Berton S, Pellizzari I, Segatto I, D'Andrea S, Armenia J, et al. p27kip1 controls H-Ras/MAPK activation and cell cycle entry via modulation of MT stability. Proc Natl Acad Sci U S A 2015;112:13916–21.
31. Fabris L, Berton S, Citron F, D'Andrea S, Segatto I, Nicoloso MS, et al. Radiotherapy-induced miR-223 prevents relapse of breast cancer by targeting the EGF pathway. Oncogene 2016;35:4914–26.

32. Chan W-C, Ho M-R, Li S-C, Tsai K-W, Lai C-H, Hsu C-N, et al. MetaMirClust: discovery of miRNA cluster patterns using a data-mining approach. Genomics 2012;100:141–8.
33. Ma L, Young J, Prabhala H, Pan E, Mestdagh P, Muth D, et al. miR-9, a MYC/MYCN-activated microRNA, regulates E-cadherin and cancer metastasis. Nat Cell Biol 2010;12:247–56.
34. Liu Y-N, Yin JJ, Abou-Kheir W, Hynes PG, Casey OM, Fang L, et al. MiR-1 and miR-200 inhibit EMT via Slug-dependent and tumorigenesis via Slug-independent mechanisms. Oncogene 2013;32:296–306.
35. Muraoka N, Yamakawa H, Miyamoto K, Sadahiro T, Umei T, Isomi M, et al. MiR-133 promotes cardiac reprogramming by directly repressing Snai1 and silencing fibroblast signatures. EMBO J 2014; 33:1565–81.
36. Yokobori T, Suzuki S, Tanaka N, Inose T, Sohda M, Sano A, et al. MiR-150 is associated with poor prognosis in esophageal squamous cell carcinoma via targeting the EMT inducer ZEB1. Cancer Sci 2013;104:48–54.
37. Pastrello C, Otasek D, Fortney K, Agapito G, Cannataro M, Shirdel E, et al. Visual data mining of biological networks: one size does not fit all. PLoS Comput Biol 2013;9:e1002833.
38. Reis PP, Waldron L, Perez-Ordonez B, Pintilie M, Galloni NN, Xuan Y, et al. A gene signature in histologically normal surgical margins is predictive of oral carcinoma recurrence. BMC Cancer 2011;11:437.
39. Beishline K, Azizkhan-Clifford J. Sp1 and the "hallmarks of cancer." FEBS J 2015;282:224–58.
40. Inman GJ. Switching TGFβ from a tumor suppressor to a tumor promoter. Curr Opin Genet Dev 2011;21:93–9.
41. Zeller C, Hinzmann B, Seitz S, Prokoph H, Burkhard-Goettges E, Fischer J, et al. SASH1: a candidate tumor suppressor gene on chromosome 6q24.3 is downregulated in breast cancer. Oncogene 2003;22:2972–83.
42. Martini M, Gnann A, Scheikl D, Holzmann B, Janssen K-P. The candidate tumor suppressor SASH1 interacts with the actin cytoskeleton and stimulates cell-matrix adhesion. Int J Biochem Cell Biol 2011;43:1630–40.
43. Yanagawa T, Yoshida H, Yamagata K, Onizawa K, Tabuchi K, Koyama Y, et al. Loss of cytokeratin 13 expression in squamous cell carcinoma of the tongue is a possible sign for local recurrence. J Exp Clin Cancer Res 2007;26:215–20.
44. Naganuma K, Hatta M, Ikebe T, Yamazaki J. Epigenetic alterations of the keratin 13 gene in oral squamous cell carcinoma. BMC Cancer 2014; 14:988.
45. White RA, Neiman JM, Reddi A, Han G, Birlea S, Mitra D, et al. Epithelial stem cell mutations that promote squamous cell carcinoma metastasis. J Clin Invest 2013;123:4390–404.
46. Leemans CR, Braakhuis BJM, Brakenhoff RH. The molecular biology of head and neck cancer. Nat Rev Cancer 2011;11:9–22.
47. Glick AB, Glick AB. The role of TGF signaling in squamous cell cancer: lessons from mouse models, the role of TGF signaling in squamous cell cancer: lessons from mouse models. J Skin Cancer 2012;2012:e249063.
48. Du L, Chen X, Cao Y, Lu L, Zhang F, Bornstein S, et al. Overexpression of PIK3CA in murine head and neck epithelium drives tumor invasion and metastasis through PDK1 and enhanced TGFβ signaling. Oncogene 2016;35:4641–52.
49. Dasgupta S, Bhattacharya-Chatterjee M, O'Malley BW, Chatterjee SK. Tumor metastasis in an orthotopic murine model of head and neck cancer: possible role of TGF-beta 1 secreted by the tumor cells. J Cell Biochem 2006;97:1036–51.
50. Jungert K, Buck A, von Wichert G, Adler G, König A, Buchholz M, et al. Sp1 is required for transforming growth factor-beta-induced mesenchymal transition and migration in pancreatic cancer cells. Cancer Res 2007;67:1563–70.